HSPI The Open Access Publisher

IJPRA ISSN 2766-2748 INTERNATIONAL JOURNAL OF PHYSICS RESEARCH AND APPLICATIONS

Research Article

3-D Current Density and Magnetic Field of 3-D MR Scanner Gradient Coil

Željko Đ Vujović*

Boulevard Save Kovačevića 20/6 81000 Podgorica, Montenegro

Abstract

The topic of this paper is to describe the 3-D current density in the windings of a 3-D coil, which fills the volume between two coaxial cylinders at a precisely defined distance from each other, and which serves to generate a magnetic field gradient in the center of the cylinder axis. The 3-D current density is considered an unknown input quantity, which is calculated from the known gradient magnetic field output. It is an inverse problem in mathematics, where the direct problems are the calculation of unknown output quantities based on known input quantities. Fourier series expansion methods in the context of cylindrical coordinates were used to describe the 3-D current density. In that case, Bessel functions are used as development components. The current densities, at each point in space, were lined up to represent current lines. Each power line is associated with a coil winding through which a current of a certain strength flows. After that, the principle of discretization of coil windings was applied. Each winding is divided into a large number of elementary segments that were considered as current elements, which create, based on Bio-Savar's law, an elementary magnetic field. In this way, the total, continuous magnetic field is broken into many elementary components, which come from different current elements. An important result of this process is that each current element can be controlled independently by a current source. This means that the output magnetic field of the gradient can be controlled by current sources, which are the input sizes, and this is what is at the core of the topic of this paper.

More Information

***Address for correspondence:** Željko Đ Vujović, Boulevard Save Kovačevića 20/6 81000 Podgorica, Montenegro, Email: etracon@t-com.me

Submitted: June 07, 2024
Approved: June 25, 2024
Published: June 28, 2024

How to cite this article: Vujović ZD. 3-D Current Density and Magnetic Field of 3-D MR Scanner Gradient Coil. Int J Phys Res Appl. 2024; 7: 086-092.

DOI: 10.29328/journal.ijpra.1001090

Keywords: Magnetic field; Gradient; 3-D coil; 3-D current density; Fourier series; Bessel functions; inverse problem

Introduction

The problem of realizing the gradient magnetic field is crucial for the operation of the MR scanner. Considerable work has been devoted to the design of gradient coils and various methods for the design of these coils. An example of those works is [1], which gives an overview of the methods for the design of gradient coils. In paper [2], an approach to the design of planar gradient coils is presented. A technique is provided that allows gradient field corrections. These corrections are made by changes in the wire paths made by the coil windings. This is why this method is called the path correction method. In the work [3] an optimal saddle coil configuration was proposed as a function of the dimensions of the region of interest, taking into account uniformity and sensitivity. To evaluate the uniformity of the magnetic field, three quantities were analyzed: nonuniformity, peak-to-peak homogeneity, and relative uniformity. Paper [4] discusses coil design by classifying it into two groups: discrete, analytical coil design, and distributed coils. In the work [5], the gradient magnetic field generated by the conventional transverse coil (Golay coil) was mapped. The calculation algorithm of the generated magnetic field was written in C-programming language, compiled by the GNU compiler collection, and was based on a forward analytical approach using the Biot-Savarot law. Paper [6] deals with the problem of overcoming the design of Golay coils and the development of so-called fingerprint coils for x- and y-gradients. In paper [7], a simple modeling based on series Fourier decomposition was proposed, which allows determining the distribution of the electric conductor to make the magnetic field homogeneous. The method is valid for flat and axisymmetric geometries. In the work [8] an innovative design method for highly uniform magnetic field coils using a Particle Swarm Optimization (PSO) algorithm was proposed. A PSO algorithm was employed to avoid obtaining parameters with a large number of decimal places. The paper [9] presents an intuitive open-source code collection for deriving the stream function from the current density on simple geometry surfaces.

The reason that led to the study of this problem came from the text "Gradient Coils" by Allen D. Elster *(https://www.mriquestions.com/gradient-coils.html).* Allen D. Elster's account is interesting but not clear enough. It is superficial. It does not sufficiently depict the essential complexity of creating a gradient magnetic field. It is shown that the solutions he presents have been overcome.

In this paper, the method of inverse solution to the problem of magnet gradient generation is presented. Based on the known output, it is shown how to realize the required input, which creates the required, target output. The target output is the desired magnetic field gradient, and the input is the 3D coils through which the 3D current density flows, creating the target output.

The gradient coil system is discretized so that each discrete element creates its own, discrete, elemental magnetic field at a chosen point in space, based on Bio-Savar's law. The total magnetic field, at that chosen point, is equal to the sum of the elementary fields at that point, produced by the discrete elements of the gradient coils.

Current density at a point in space

Current density at an arbitrary point in space is defined as the amount of current that passes through that point at a given moment. At an arbitrary point in space (r′,θ′,z′), the magnitude of the current density vector J(r′,θ′,z′) is expressed in the following way:

ΔQ – charge of one particle,

N′ – particle density volume, (number of particles in unit volume)

ρ = Δq·N′ – volumetric charge density

---

dq = ΔQ·N′·dv

dv = ΔS·dl

dl = v·dt

dq = ΔQ·N′·v·dt/:dt

Δi = (dq/dt) = ΔQ·N′·v·Δs/:Δs

J = (Δi/Δs) = ΔQ·N′·v

ΔQ·N′ = ρ

$\boldsymbol{J} = \rho\cdot\boldsymbol{v}$

The current density vector J is proportional to the speed of electricity movement v. The electric current is a consequence of the action of the electric field E. So, there is a proportionality (v ~ E) between the vector v and the vector E. It follows from this:

$\boldsymbol{J} = \sigma\boldsymbol{E}\ [J(r',\theta',z') = \sigma\boldsymbol{E}(r',\theta',z')]$

σ is the conductivity of the medium in which the current is established due to the field ***E***.

This is Ohm's law in differential form. The current density at a point in space is proportional to the field strength at that point [10].

Model 3–D coil gradient

A 3-D gradient coil is defined to exist within the volume between two cylinders of length 2L, with inner radius a and outer radius b, lying coaxially with the z-axis and centered at z=0. In this volume, there is an unknown current density vector $\boldsymbol{J}(r',\theta',z')$ that needs to be determined to induce the desired target magnetic field in the inner region. The inner target region is a spherical volume of the appropriate diameter (DSV – Diameter of Sphere Volume) with a center at zero and radius *c*.

The outer target region is the surface of a cylinder of radius d>b, length 2L, on which the induced field should be minimized. The three-dimensional current density in the 3-D gradient coil model $\boldsymbol{J}(r',\theta',z')$ is considered as a complex quantity. Therefore, it is decomposed into the Fourier series [11], into its "spectral components", to facilitate its analysis. The point (r',θ',z') is the source point in the current density volume space.

To enable the search for a general solution, it was assumed that the components of the current density vector are: periodic in θ from -π to π, periodic in z′ from –L to 3L, and periodic in r′ from a to (2b-a). Additional current density constraints include a zero radial component at the inner and outer coil surfaces $\boldsymbol{J}(a',\theta',z')= \boldsymbol{J}(b',\theta',z')=0$ and a zero axial component at the ends $J_z(r', \theta',-L)=J_z(r',\theta', L)=0$. In addition to the above, three components of the current density vector satisfy the time-independent continuity equations: ···· $\nabla\boldsymbol{J}=0$ [12].

The continuity equation in electromagnetics expresses the law of conservation of electric charge and relates changes in the electric charge density to the divergence of the electric current density. The general forms of the continuity equation are:

$\nabla\cdot\boldsymbol{J} = -(\partial\rho/\partial t)$

J – current density (vector) per unit area,

ρ – electric charge density (scalar) per unit volume,

(∂ρ/∂t) – change in electric load density over time,

∇·***J*** – current density divergence.

The continuity equation states that the change in electric charge density in a volume over time must be equal to the negative value of the divergence of the current density in that volume. In other words, if the load density changes, it must be due to the current entering or leaving that volume.

When the equation of continuity in electromagnetism is equal to zero, it means that there is no change in the electric charge density in time at a certain place, that is, the charge density is constant in time. When the continuity equation is zero, it means that there is no net flow of charge within that region. The amount of charge remains constant over time.

This is the case, for example, in situations where the current density is distributed evenly [11,12] (Figure 1).

The complex components of the current density vector $\boldsymbol{J}(r',\theta',z')$ were chosen to be:

$$J_z(r',\theta',z') = \sum_{n=1}^{N}\cdot\sum_{m=1}^{M}\cdot\sum_{k}^{K}=1\cdot \left\{ \begin{array}{l} \cos[\frac{k\pi(r'-a)}{b-a}]\cdot\sin[\frac{n\pi(z'+L)}{2L}]\cdot\left[A_{mnk}\cdot\cos m\theta' + B_{mnk}\cdot\sin\theta'\right] + \\ +\sin[\frac{k\pi(r'-a)}{b-a}\cdot\sin[\frac{n\pi(z'+L)}{2L}]\cdot\left[C_{mnk}\cdot\cos\theta' + D_{mnk}\cdot\sin m\theta\right] \end{array} \right\}$$

$$J_r(r',\theta',z') = \sum_{n=1}^{N}\cdot\sum_{m=1}^{M}\cdot\sum_{k}^{K}=1\cdot \left\{ \begin{array}{l} \sin[\frac{k\pi(r'-a)}{b-a}\cdot\cos[\frac{n\pi(z'+L)}{2L}]\cdot\left[F_{mnk}\cdot\cos m\theta' + G_{mnk}\cdot\sin\theta'\right] + \\ +\sin[\frac{k\pi(r'-a)}{b-a}\cdot\sin\cdot[\frac{n\pi(z'+L)}{2L}\cdot\left[P_{mnk}\cdot\cos\theta' + Q_{mnk}\cdot\sin m\theta'\right] \end{array} \right\}$$

$$J_\theta(r',\theta',z') = -\sum_{n=1}^{N}\cdot\sum_{m=1}^{M}\cdot\sum_{k}^{K}=1\cdot\frac{1}{m}$$

$$\left\{ \begin{array}{l} \left[\sin[\frac{k\pi(r'-a)}{b-a}+\frac{k\pi r'}{b-a}\cos\left(\frac{k\pi(r'-a)}{b-a}\right)\right]\cos[\frac{n\pi(z'+L)}{2L}]\cdot \\ \left[F_{mnk}\cdot\sin m\theta' - G_{mnk}\cdot\cos\theta'\right] + \\ \sin\left[\frac{k\pi(r'-a)}{b-a}\right] + \frac{k\pi r'}{b-a}\cdot\cos\left[\frac{k\pi(r'-a)'}{b-a}\right]\cdot\sin\left[\frac{n\pi(z'+L)}{2L}\right]\cdot \\ \left[P_{mnk}\cdot\cos\theta' + Q_{mnk}\cdot\sin m\theta'\right] \\ +r'\cos[\frac{k\pi(r'-a)}{b-a}]\cdot\frac{n\pi}{2L}\cdot\cos\left[\frac{n\pi(z'+L)}{2L}\right]\cdot \\ \left[A_{mnk}\cdot\sin m\theta' - B_{mnk}\cdot\cos m\theta'\right] + \\ r'\sin\left[\frac{k\pi(r'-a)}{b-a}\right]\cdot\frac{n\pi}{2L}\cdot\cos\left[\frac{n\pi(z'+L)}{2L}\right]\cdot \\ \left[C_{mnk}\cdot\sin m\theta' - D_{mnk}\cdot\cos m\theta'\right] \end{array} \right\}$$

The equations for $\boldsymbol{J}_z(r',\theta',z')$, $\boldsymbol{J}_r(r',\theta',z')$ and $\boldsymbol{J}_\theta(r',\theta',z')$ include eight sets of unknown 3-D current density coefficients: A_{mnk}, B_{mnk}, C_{mnk}, D_{mnk}, F_{mnk}, G_{mnk}, P_{mnk} and Q_{mnk} (m=1:M, n=1:N, k=1:K), which should be determined [13].

Fourier transformation

The Fourier transformation is based on the idea that the entire space with "normal axes" is transformed into a space in which the new orthogonal axes are sine and cosine waves and their higher harmonics. The signal, which we transform, is only one point (local vector), and the values on each axis are the amplitudes of each harmonic individually *(A0, A1, ... AN)* [14].

Applying Euler's identity formula: $e^{j\omega} = \cos\omega + i\sin\omega$,

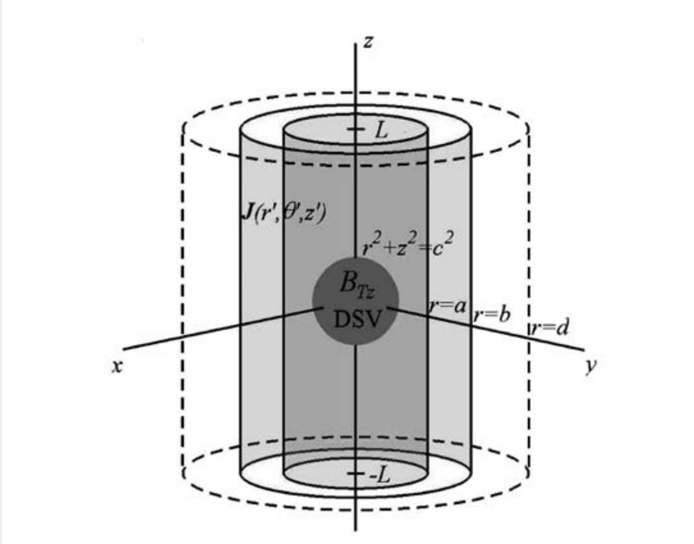

Figure 1: The model used to describe 3-D gradient coils: a cylindrical volume with inner radius a, outer radius b, and length 2L, lying coaxially with the z-axis, contains a 3-D current density *J(r',θ',z')*. There is a spherical inner target region (DSV) of radius c, centered at the starting point, the intersection of the coordinate axes, which encloses the desired gradient target field $\boldsymbol{B}_{Tz}$, and an outer cylindrical region of radius d and length 2L, where the zero field is desired. – Creative Commons License CC BY – NC – SA 4.0 [13].

expressions are obtained:

$$\cos(x) = \frac{1}{2}\left(e^{ix} + e^{-ix}\right) \; i \sin(x) = \frac{1}{2i}\left(e^{ix} - e^{-ix}\right)$$

e is Euler's number - the basis of the natural algorithm, i is an imaginary unit, and x is an angle expressed in radians.

An arbitrary periodic continuous function is expressed by the sum of trigonometric functions (sine and cosine). As a final expression, the definition of the Fourier series is obtained:

$$f_N(t) = \sum_{n=-N}^{n=N} Cn.e^{in\omega t} \quad [14]$$

Fouries–bessel series

Bessel functions are solutions of the Bessel differential equation:

x2(dy2/dx2) + x(dy/dx) + (x2−υ2)y=0

υ = const, an arbitrary real or complex number, is called the order of the Bessel function [15].

Bessel functions are also called cylindrical functions. The curves of these functions resemble sinusoids whose amplitude decreases [16].

Cylindrical functions of the first kind are solutions of Bessel's differential equation, which are finite in the coordinate origin (x=0), for negative integer values υ, and are infinite when x tends to zero, for negative non-integer values υ [16].

Cylindrical functions of arbitrary order, if υ is not an integer, have a general solution

$c_1 J\upsilon + c_{-1} J_{-\upsilon}$ [17,18]

J±υ are the so-called cylindrical functions of the first kind.

Cylindrical functions of the first kind have the form:

$$J_\upsilon(z) = \left(\frac{z}{2}\right)^{\upsilon} \sum_{m=0}^{\infty} \cdot \frac{(-1)^m}{m!\Gamma(\upsilon+m+1)} \cdot (\frac{z}{2})2m \quad [17]$$

Γ is the Gamma function, the transcendental function Γ(z) that expands the values of the factorial z! to any complex number. It is written Γ(z)=(z–1)! [19,20].

Cylindrical functions of the second kind have the form:

$$J_\upsilon(z) = \frac{J\upsilon(z)\cos\upsilon\pi - J - \upsilon(z)}{\sin\upsilon\pi} \text{ za } \upsilon \in Z \quad [18]$$

The function f is expressed as a string:

$$f(x) = \sum_{m=1}^{\infty} c_m J_\upsilon\left(x_m^{(\upsilon)}\right), \quad 0 < x < a$$

f is a function given in the interval (0, a), Jυ is a cylindrical function of order υ > – 1/2, and $x_m(\upsilon)$ are positive zeros of J_υ taken in increasing order. The coefficients c_m have the values given by the expression in [21].

Bio-savar's law [22]

Bio-Savar's law gives a quantitative relationship between the electric current and the magnetic field B produced by that current. The current in the loop produces magnetic field lines *B*, and these magnetic field lines form loops around the current in the loop. In differential form, Bio-Savar's law expresses the partial contribution *dB* of a small segment of the conductor to the total field *B* of the current in the conductor. For a conductor segment of length dl and orientation dl, through which current I flow, Bio-Savar's law has the form:

$$dB = \frac{\mu}{4\pi} \cdot \frac{idlx\hat{\tau}}{r \cdot r}$$

μ is the permeability of the free space, *I* – current measured in amperes, *dl* – differential length vector, ***Idl*** is the differential current element, $\hat{r}$ – unit vector of the distance from the current element to the field point, ***r*** – the distance from the current differential element to the field point.

The equation expressing Bio-Savar's law is illustrated, in Figure 2, for a small segment of wire through which current flows. A small segment of wire lies at the origin along the x-axis. Comparing dB at points 1 and 2 shows an inverse quadratic dependence of field size with distance. Vectors 1, 3, and 4, which are all equidistant from dl, show the direction of dB in a circle around the wire. In position 1, the field contribution dB1 is vertical to the direction of the current and the vector r1. Plots 1, 5, 6, and 7 illustrate the angular dependence of the magnitude of dB at a point. The magnitude dB varies as the sine of the angle between dl and r̂. (r̂ is in the direction from dl to point.) It is largest at 900 to dl and decreases to zero for locations in line with dl. The magnetic field of the current in the loop or coil is obtained by summing the individual partial contributions of all circuit segments, taking into account the vector nature of the field.

The expression for the magnetic field B at a distance r from a long straight wire with a current I is:

$$B = \frac{\mu I}{2\pi r} \cdot \grave{e}$$

θ is the only vector that points in a circle around the wire. So, the value of the magnetic field B at a point nearby is directly proportional to the value of the current *I*, and inversely proportional to the distance r from the wire to the given point.

The magnetic induction vector ***B(r)*** at the field point ***(r)***, induced by the current density ***J(r')*** existing at the source points ***(r')*** contained in the volume V', is given by Bio-Savar's law through conducting volumes [18] (Figure 3).

Each coil winding, individually, is divided into elementary segments. Each of these segments can be controlled, independently of the others, by a source of electric current. In this way, the continuous magnetic field, at each point, is broken into components. Each of these components is a sum of elementary magnetic fields created by elementary segments of the coil.

$r'_{wq}(x'_{wq}, y'_{wq}, z'_{wq})$ – position vector for each elemental segment of the coil

w – ordinal number of coil windings,

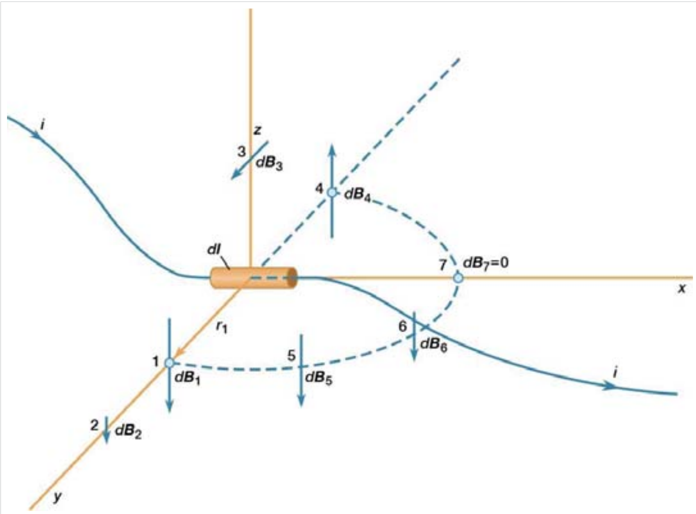

Figure 1: A magnetic field produced by a small section of wire with an electric current I. – Creative Commons License CC BY – NC – SA 4.0 [18]

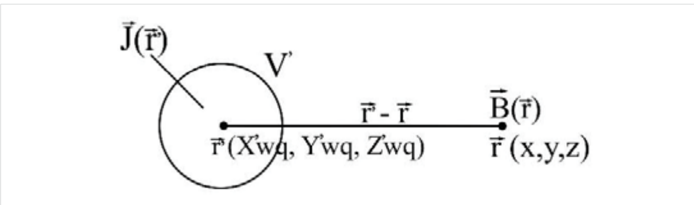

Figure 3: Elementary magnetic field ***dB***, at a point in space ***r***, is induced by the elementary current density ***J(r')*** that exists at the source point ***r'*** in the volume V'.

q – sequence number of the current segment,

$\boldsymbol{r}(x,y,z)$ – position vector for all points of interest.

For a discretized system of W windings of a coil, such that a current I_w flows through each discrete segment (w=1:W), and the position of the segment is described by the coordinates $(x'_{wq}, y'_{wq}, z'_{wq})$ $(q=1:Q_w)$, the magnetic induction vector becomes expression:

$$\Delta\mathbf{B}(\mathbf{r}) = \frac{\mu}{4\pi}\cdot[\Delta S'_{wq} x(r_{wq} - \mathbf{r}) / R^3{}_{wq}]$$

$$R^3{}_{wq} = [(x'_{wq}-x)^2 + (y'_{wq}-y)^2 + (z'_{wq}-z)]^{1/2}$$

Each winding of the coil individually represents a current line, and the elemental segment of the coil is a discretized segment of the current line (Figure 4).

$$\Delta\mathbf{S}'_{wq} = \Delta x'_{wq} \cdot \boldsymbol{e}_x + \Delta y'_{wq} \cdot \boldsymbol{e}_y + \Delta z'_{wq} \cdot \boldsymbol{e}_z$$

$\Delta\mathbf{S}'_{wq}$ – discretized current line segment,

$\boldsymbol{e}_x$, $\boldsymbol{e}_y$, and $\boldsymbol{e}_z$ are unit vectors along the usual axes of the Cartesian coordinate system,

$x'_{wq}=(x'_{wq+1}-x_{wq})$, $(\Delta y'_{wq}=y'_{wq+1}-y_{wq})$, $(\Delta z'_{wq}=\Delta z'wq+1-\Delta z'wq)$ are the values of individual elementary components.

For this discretized system of W coils, each divided into q segments, Bio-Savar's law takes the form:

$w=1$, $q \in [1,Q_1]$;

$$\frac{\mu_0}{4\pi}\left\{\frac{\Delta S_{11}{}' x(r_{11}{}' - r)}{R_{11}^3} + \frac{\Delta S_{12}{}' x(r_{12}{}' - r)}{R_{12}^3} + \cdots + \frac{\Delta S_{1Q1}{}' x(r_{1Q1}{}' - r)}{R_{1Q1}^3}\right\}$$

$$R_{11}=[(x_{11}{}'-x)^2+(y_{11}{}'-y)^2+(z_{11}{}'-z)]^{1/2} + \cdots$$

$w=2$, $q \in [1,Q_2]$

$$\frac{\mu_0}{4\pi}\left\{\frac{\Delta S_{21}{}' x(r_{21}{}' - r)}{R_{21}^3} + \frac{\Delta S_{22}{}' x(r_{22}{}' - r)}{R_{22}^3} + \cdots + \frac{\Delta S_{2Q2}{}' x(r_{2Q2}{}' - r)}{R_{2Q2}^3}\right\}$$

$$R_{21}=[(x_{21}{}'-x)^2+(y_{21}{}'-y)^2+(z_{21}{}'-z)]^{1/2} + \cdots$$

$w=3$, $q \in [1,Q_3]$;

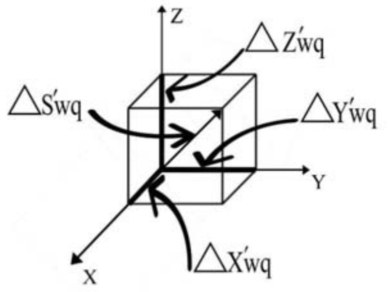

Figure 4: Vector representation of the discretized element of the current line S'_{wq}.

$$\frac{\mu_0}{4\pi}\left\{\frac{\Delta S_{31}{}' x(r_{31}{}' - r)}{R_{31}^3} + \frac{\Delta S_{32}{}' x(r_{32}{}' - r)}{R_{32}^3} + \cdots + \frac{\Delta S_{3Q3}{}' x(r_{3Q3}{}' - r)}{R_{3Q3}^3}\right\}$$

$$R_{11}=[(x_{31}{}'-x)^2+(y_{31}{}'-y)^2+(z_{31}{}'-z)]^{1/2} + \cdots$$

.

.

.

$w=W$, $q \in [1,Q_W]$;

$$\frac{\mu_0}{4\pi}\left\{\frac{\Delta S_{w1}{}' x(r_{w1}{}' - r)}{R_{w1}^3} + \frac{\Delta S_{w2}{}' x(r_{w2}{}' - r)}{R_{w2}^3} + \cdots + \frac{\Delta S_{wQw}{}' x(r_{wQw}{}' - r)}{R_{wQw}^3}\right\}$$

$$R_{W1}=[(x_{W1}{}'-x)^2+(y_{W2}{}'-y)^2+(z_{WQW}{}'-z)]^{1/2} + \cdots$$

Are the radii R_{wq} calculated individually for each segment or is the average value of the radius of all segments of one coil estimated?

The axial component of the magnetic field, calculated based on Bio-Savar's law, is expressed, using currents J_r and J_z, in cylindrical coordinates, as:

$$B_z=(\mu_0/4\pi)=(J_r \cdot r'/r'^2)\cdot dr'\cdot d\theta\cdot dz + (\mu_0/4\pi)=(J_z \cdot r'/r'^2)\cdot dr' d\theta' \cdot dz$$

The first integral is the contribution of the radial current component J_r, and the second integral is the contribution of the axial current component J_z. Both integrals integrate over the entire volume containing the current. [19]

Discussion

The first significant contribution of this paper is the reminder that the current density at an arbitrary point in space is proportional to the strength of the electric field at that point. This leads us to recall that the electric field is created by an external source of electricity supply. In this way, we become aware of the important fact that the phenomenon we are considering in this paper originates from an external source of electric current, which is necessary for the existence of the considered phenomenon.

In the three-dimensional model of the gradient coil, in Figure 1, the starting point is the output data, that is, the resultant gradient of the magnetic field, which should be obtained. The goal is to discover the causal relationship, that is, the input data that led to those results, the output data. It is an inverse problem in mathematics, which is, in principle, more complex than the direct problem. In this case, information that is not directly available through measurement or observation is reconstructed. In this context, we highlighted the notion of cylindrical functions, which are used in problems with cylindrical symmetry. Such a problem is considered in this paper. The idea is to express the functions of the electromagnetic field in a cylindrical structure in the form of a Fourier-Bessel series.

The known output data, the induced magnetic field in the target, spherical volume, led to, in electromagnetics, the logical assumption that the cause of that induced magnetic field, current, is a complex three-dimensional current density, characterized by a vector at each source point, described by cylindrical coordinates, **J**(r',θ',z'). Finding the assumed complex current density in this way required the introduction of additional restrictions on it, to facilitate solving the problem.

In the work [11], the authors assumed very complex expressions for three cylindrical components of the current density, which contain eight sets of unknown coefficients, which need to be determined.

The complexity of the representation of the current density components was considered by decomposing them into constituent components in the form of the Fourier series in the context of cylindrical coordinates. In this context, the components of the Fourier series are Bessel functions, and the Fourier coefficients determine the share of each term in the development of the function. Specifying the development of the current density function in the Fourier series using Bessel functions is a very interesting and significant contribution of this paper.

The information about the source point in space, characterized by the current density vector **J**(r', θ', z'), led us to consider the model from Figure 1 and the cylindrical volume bounded by radii a and b, as a set of a huge number of such source points, connected in series – current lines. Each current line has its conductor, a coil, through which it flows. A complete coil consists of W coils, and each of these coils is divided into q segments. In this way, the physical equivalents of the original points were created. The coil is visualized so that it is considered a set of different, unrelated elements. Each of these elements, based on Bio-Savar's law, creates its magnetic field. The total magnetic field is the sum of all elementary fields created in this way. The meaning of this entire procedure is that each of the resulting elements, the segments of the coil, can be controlled separately, with a separate power supply. In this way, the magnetic field, or magnetic induction, at any point in space, is controlled by a special source of electric current. This is also the solution to our inverse problem, which we consider in this paper: we received input data, electric current sources, which create the desired output, and a magnetic field within the central spherical region of a cylindrical 3-D gradient coil. It is a theoretical solution, based on which a practical solution is realized.

The key factors affecting the distribution of the magnetic field generated by the 3D gradient of the coil are the geometric shape and size of the coil, the total number of coils and their arrangement (coil density), as well as the strength of the current flowing through the coil. Induced currents in the conducting components of the MRI system can distort the gradient field. This effect is mitigated by using actively shielded gradient circuits and eddy current compensation techniques. The magnetic field distribution generated by a 3D gradient coil is a complex interaction of design choices, material properties, external influences, and operating conditions.

The optimal 3D current density distribution should allow the gradient coil to achieve high performance without high power consumption and heat generation. High performance means that the generated magnetic fields are linear and predictable.

This paper sets the framework within which the Bio-Savar technique and optimization method are considered, which involves using the Bio-Savar law to directly calculate the magnetic field produced by a given current distribution. By iteratively adjusting the current distribution and recalculating the resulting field, the optimization process can fine-tune the coil design to achieve the desired field characteristics [23].

Conclusion

The contribution of this paper is particularly significant to the author's published results because it provides a completely different approach for the design and implementation of MR scanner gradient coils. In the original papers, Maxwell's pair of coils and saddle–Golay coils were specified for generating a gradient magnetic field. Such an approach to creating magnetic gradients is considered outdated. This paper highlights that.

A significant contribution of the work is the description of the mathematical modeling of the phenomenon of the creation of the volumetric current density, which produces the target magnetic gradient. As a consequence, a discretized gradient coil winding system is described, in which each discretized element produces, based on Bio-Savar's law, a discretized magnetic gradient element, and the total gradient is the sum of all those elementary gradients.

It is puzzling how the authors in [11] assumed the expressions for the cylindrical current components $J_z(r',\theta',z')$, $J_r(r',\ \theta',z')$, and $J_\theta(r',\ \theta',z')$) with sets of coefficients to be determined.

The contribution of the work is the theoretical consideration of the development of the current density components into Fourier series in the context of cylindrical coordinates, using Bessel functions as development components.

A challenge for future work may be to consider the process of regularization and optimization of the coil current and the results processed and obtained by the authors in the paper [11].

This work inspired questions that would be worth answering:

1. How does the three-dimensional (3D) distribution of current within the gradient coil affect scanner performance?

2. What factors affect the distribution of the magnetic field generated by the 3D gradient MR scanner coil?

3. What is the relationship between the 3D current density and the strength of the resultant magnetic field inside the gradient coil?

4. Are there any optimization techniques and methods currently in use to achieve an ideal 3D current density distribution in MR scanner gradient coils?

In the discussion, we gave answers to these questions, but a studious consideration of these insights and answers to them is a challenge for some, possible, future work. The consideration of very different optimization procedures seems particularly complex and, because of this, as well as its importance for application, deserves special attention.

Acknowledgement

The author declares that, in this work, he partially used content generated by Artificial Intelligence.

I. He used the ChatGPT software tool, version 3.5;

II. The ChatGPT tool was used by asking questions related, primarily, to solving optimization problems. It represented a certain kind of challenge and tested whether and how well the AI tools were informed about the optimization problem and the techniques and methods to solve it.

Apart from the optimization problem, the author used the same Artificial Intelligence tool, with the same, previously found goal, to consider the development of functions in the Fourier series and the use of Bessel functions for that development. He received information, which, he believes, should not be neglected.

III. After using the AI tool ChatGPT, the author reviewed and edited the responses he received, so that he takes responsibility for the bias that could be introduced by the AI.

IV. The author assumes full responsibility for the content of this paper.

References

1. Turner R. Gradient coil design: a review of methods. Magn Reson Imaging. 1993;11(7):903-20. doi: 10.1016/0730-725x(93)90209-v. PMID: 8231676.
2. Veght V, Zhaw H, Galloway GJ, Doddrell DM, Breton IM. The design of planar gradient coils. Part I: A winding path correction method. Concepts Magn Reson Part B Magn Reson Eng. 2005;27B(1):17-24. doi: 10.1002/cmn.b.20049.
3. Garrido Salamon CE, Gea Vidoto EL, Martins MJ, Tannus A. Optimization of saddle coils for magnetic resonance imaging. Braz J Phys. 2006 Mar;36(1A).
4. Michael Poole "Improved Equipment and Techniques for Dynamic Shimming and High Field MRI", Thesis submitted to the University of Nottingham for the degree of Doctor of Philosophy, August 2007.
5. Rashdy Shah Ahmad, Amirudin Bin Sharri, Chew Teong Han, "Magnetic Field Simulation of Golay Coil", Journal of Fundamental Sciences, 30 October 2008.
6. Schmitt F, Schall K, "The Gradient System", Proc. Intl. Soc. Mag. Reason. Med. 21: 2013.
7. Coillet C, Nativel E, Zanca M, Goze–Bas C. The magnetic field homogeneity of coils using the space harmonics superposition of the current density distribution. J Sens Sens Syst. 2016;5:401-408. Available from: www.j.-sens-sens-system.net/5/401/2016. doi: 10.5194/jsss-5-401-2016.
8. Wu W, Zhou B, Lin Z, Wang J, Pang H, Chen L, Quan W, Lin G. Design of highly uniform magnetic field coils based on a particle swarm optimization algorithm. IEEE Access. 2019 Sep 16. doi: 10.1109/ACCESS.2019.29333608.
9. Latin S, Jia F, Amrein P, Zaitsew M. Methods: Of stream functions and thin wares: An intuitive approach to gradient coil design. Front Phys. 2021;9:699468. doi: 10.3389/tphy.2021.699468.
10. Conduction current. Current density. https://www.ucg.ac.me/skladište/blog-7790/objava-63790/fajlovi/PredavanjeII.pdf (Accessed: April 16, 2024).
11. Continuity equation – Differential form. https://en.wikipedia.org/wiki/Continuity_equation (Accessed June 21, 2024).
12. While PT, Forbes LK, Grozier S. 3-D gradient coil design - initial theoretical framework. IEEE Trans Biomed Eng. 2009 Apr;56(4).
13. Huge S. Current, continuity equation, resistance and Ohm's law. Massachusetts Institute of Technology Department of Physics, 8.022 spring 2005, Lecture 7.
14. While PT, Forbes LK, Grozier S. 3-D gradient coil design – initial theoretical framework. IEEE Trans Biomed Eng. 2009 Apr;56(4).
15. Fourier's row. https://sr.wikipedia.org/wiki/Fourieov_red. Creative Commons License CC-BY-NC– SA 4.0 (Accessed: April 7, 2024).
16. Encyclopedia of Mathematics. Bessel equation. https://encyclopediaofmath.org/wiki/Bessel_equation.
17. Besselove funkcije. Hrvatska enciklopedija, mrežno izdanje, Leksikografski zavod Miroslav Krleža, 2013-2024. https://enciklopedija.hr/clanak/besselove-funkcije (Accessed April 22, 2024).
18. Encyclopedia of Mathematics. Cylinder functions. https://encyclopediaofmath.org/wiki/Cylinder_functions.
19. Encyclopedia of Mathematics. Cylinder functions of arbitrary order. https://encyclopediaofmath.org/wiki/Cylindar_functions#Cylinder_functions_of_arbitrary_order.
20. Encyclopedia of Mathematics. Gamma function. https://encyclopediaofmath.org/wiki/Gama-function.
21. Gama-funkcija. Hrvatska enciklopedija, mrežno izdanje, Leksikografski zavod Miroslav Krleža, 2013-2024. https://www.ecikloedija.hr/gama-funkcija (Accessed April 22, 2024).
22. Encyclopedia of Mathematics. Fourier Bessel series. https://encyclopediaofmath.org/wiki/Fourier_Bessel_series.
23. BRITANIKA, The Editors of Enciklopedia, Biot-Savarot-law, Enciklopedia Britanika, February, 2024. https://www.britanika.com/science/Biot-Savarot-law Creative Commons Licenses CC-BY-NC– SA 4.0 (28. 05. 2024.)